

# Predictions of $pp, \bar{p}p$ total cross section and $\rho$ ratio at LHC and cosmic-ray energies

Keiji Igi<sup>a</sup> and Muneyuki Ishida<sup>b</sup>

<sup>a</sup>*Theoretical Physics Laboratory, RIKEN, Wako, Saitama 351-0198, Japan*

<sup>b</sup>*Department of Physics, Meisei University, Hino, Tokyo 191-8506, Japan*

---

## Abstract

We propose to use rich informations on the  $pp, \bar{p}p$  total cross sections  $\sigma_{\text{tot}}$  below  $N(\sim 10)\text{GeV}$  in order to predict the total cross section and  $\rho$  ratio at very high energies. Using the FESR as a constraint for high energy parameters, we search for the simultaneous best fit to the data points of  $\sigma_{\text{tot}}$  and  $\rho$  ratio up to some energy (e.g., ISR, Tevatron) to determine the high-energy parameters. We then predict  $\sigma_{\text{tot}}$  and  $\rho$  in the LHC and high-energy cosmic-ray regions. Using the data up to  $\sqrt{s} = 1.8\text{TeV}$  (Tevatron), we predict  $\sigma_{\text{tot}}^{pp}$  and  $\rho^{pp}$  at the LHC energy ( $\sqrt{s} = 14\text{TeV}$ ) as  $106.3 \pm 1.9\text{mb}$  and  $0.126 \pm 0.004$ , respectively. The predicted values of  $\sigma_{\text{tot}}$  in terms of the same parameters are in good agreement with the cosmic-ray experimental data up to  $P_{\text{lab}} \sim 10^{8\sim 9}\text{GeV}$ .

*Key words:*  $pp, \bar{p}p$  total cross section,  $\rho$  ratio, FESR, LHC

*PACS:* 13.85.Lg, 14.20.Dh

---

Recently[1], we have proposed to use rich informations on  $\pi p$  total cross sections below  $N(\sim 10 \text{ GeV})$  in addition to high-energy data to discriminate whether these cross sections increase like  $\log \nu$  or  $\log^2 \nu$  at high energies[2]. The FESR which was derived in the spirit of the  $P'$  sum rule[3] as well as the  $n = 1$  moment FESR([4], [5]) have been required to constrain the high-energy parameters. We then searched for the best fit of  $\sigma_{\text{tot}}^{(+)}$  above  $70\text{GeV}$  in terms of high-energy parameters constrained by the two FESR. We then arrived at the conclusion that our analysis prefers the  $\log^2 \nu$  behaviours consistent with the Froissart-Martin unitarity bound[6].

As for the  $\bar{p}p$  and  $pp$  total cross sections, there are a lot of data including cosmic-ray data up to  $\sqrt{s} \sim$  several times of  $10^4\text{GeV}$  compared with data up to  $\sqrt{s} \sim 30\text{GeV}$  for  $\pi N$  scattering. Therefore, it is very valuable if one could investigate the high-energy behaviours at LHC and cosmic-ray regions[8] using the similar approach as ref. [1].

(The purpose of this Letter): The purpose of this Letter is to predict  $\sigma_{\text{tot}}^{(+)}$ , the  $\bar{p}p$ ,  $pp$  total cross sections and  $\rho^{(+)}$ , the ratio of the real to imaginary part of the forward scattering amplitude at the LHC and the higher-energy cosmic-ray regions, using the experimental data for  $\sigma_{\text{tot}}^{(+)}$  and  $\rho^{(+)}$  for  $70\text{GeV} < P_{\text{lab}} < P_{\text{large}}$  as inputs. We first choose  $P_{\text{large}} = 2100\text{GeV}$  corresponding to ISR region ( $\sqrt{s} \simeq 60\text{GeV}$ ). Secondly we choose  $P_{\text{large}} = 2 \times 10^6\text{GeV}$  corresponding to the Tevatron collider ( $\sqrt{s} \simeq 2\text{TeV}$ ). In a recent paper, Block and Halzen[7] emphasized the importance of  $\rho$  for the evidence for saturation of the Froissart-Martin bound[6]. We also use the  $\rho$  ratio as input data in addition to FESR as a constraint. We searched for the simultaneous best fit of  $\sigma_{\text{tot}}^{(+)}$  and  $\rho^{(+)}$  in terms of high-energy parameters  $c_0, c_1, c_2$  and  $\beta_{P'}$  constrained by the FESR. It turns out that the prediction of  $\sigma_{\text{tot}}^{(+)}$  agrees with  $pp$  experimental data at these cosmic-ray energy regions[8] within errors in the first case ( ISR ). It has to be noted that the energy range of predicted  $\sigma_{\text{tot}}^{(+)}, \rho^{(+)}$  is several orders of magnitude larger than the energy region of  $\sigma_{\text{tot}}^{(+)}, \rho^{(+)}$  input (see Fig. 1). If we use data up to Tevatron (the second case), the situation is much improved (see Fig. 2).

FESR(1): Firstly we derive the FESR in the spirit of the  $P'$  sum rule [3]. Let us consider the crossing-even forward scattering amplitude defined by

$$F^{(+)}(\nu) = \frac{f^{\bar{p}p}(\nu) + f^{pp}(\nu)}{2} \quad \text{with} \quad \text{Im } F^{(+)}(\nu) = \frac{k}{4\pi} \sigma_{\text{tot}}^{(+)}(\nu) . \quad (1)$$

We also assume

$$\begin{aligned} \text{Im } F^{(+)}(\nu) &= \text{Im } R(\nu) + \text{Im } F_{P'}(\nu) \\ &= \frac{\nu}{M^2} \left( c_0 + c_1 \log \frac{\nu}{M} + c_2 \log^2 \frac{\nu}{M} \right) + \frac{\beta_{P'}}{M} \left( \frac{\nu}{M} \right)^{\alpha_{P'}} \end{aligned} \quad (2)$$

at high energies ( $\nu > N$ ). We have defined the functions  $R(\nu)$  and  $F_{P'}(\nu)$  by replacing  $\mu$  by  $M$  in Eq. (3) of ref.[1].

Since the amplitude is crossing-even, we have

$$\begin{aligned} R(\nu) &= \frac{i\nu}{2M^2} \left\{ 2c_0 + c_2 \pi^2 + c_1 \left( \log \frac{e^{-i\pi}\nu}{M} + \log \frac{\nu}{M} \right) \right. \\ &\quad \left. + c_2 \left( \log^2 \frac{e^{-i\pi}\nu}{M} + \log^2 \frac{\nu}{M} \right) \right\} , \end{aligned} \quad (3)$$

$$F_{P'}(\nu) = -\frac{\beta_{P'}}{M} \left( \frac{(e^{-i\pi}\nu/M)^{\alpha_{P'}} + (\nu/M)^{\alpha_{P'}}}{\sin \pi \alpha_{P'}} \right) , \quad (4)$$

and subsequently obtain

$$Re \ R(\nu) = \frac{\pi\nu}{2M^2} \left( c_1 + 2c_2 \log \frac{\nu}{M} \right) , \quad (5)$$

$$Re \ F_{P'}(\nu) = -\frac{\beta_{P'}}{M} \left( \frac{\nu}{M} \right)^{0.5} , \quad (6)$$

substituting  $\alpha_{P'} = \frac{1}{2}$  in Eq. (4). Let us define

$$\tilde{F}^{(+)}(\nu) = F^{(+)}(\nu) - R(\nu) - F_{P'}(\nu) \sim \nu^{\alpha(0)} \ (\alpha(0) < 0) . \quad (7)$$

Using the similar technique to ref.[1], we obtain

$$\begin{aligned} Re \ \tilde{F}^{(+)}(M) &= \frac{2P}{\pi} \int_0^\infty \frac{\nu Im \ \tilde{F}^{(+)}(\nu)}{k^2} d\nu \\ &= \frac{2P}{\pi} \int_0^M \frac{\nu}{k^2} Im \ F^{(+)}(\nu) d\nu + \frac{1}{2\pi^2} \int_0^{\bar{N}} \sigma_{\text{tot}}^{(+)}(k) dk \\ &\quad - \frac{2P}{\pi} \int_0^N \frac{\nu}{k^2} \left\{ Im \ R(\nu) + \frac{\beta_{P'}}{M} \left( \frac{\nu}{M} \right)^{0.5} \right\} d\nu , \end{aligned} \quad (8)$$

where  $\bar{N} = \sqrt{N^2 - M^2} \simeq N$ . Let us call Eq. (8) as the FESR(1).

(FESR(2)): The second FESR corresponding to  $n = 1$  [5] is:

$$\begin{aligned} &\int_0^M \nu Im \ F^{(+)}(\nu) d\nu + \frac{1}{4\pi} \int_0^{\bar{N}} k^2 \sigma_{\text{tot}}^{(+)}(k) dk \\ &= \int_0^N \nu Im \ R(\nu) d\nu + \int_0^N \nu Im \ F_{P'}(\nu) d\nu . \end{aligned} \quad (9)$$

We call Eq. (9) as the FESR(2) which we use in our analysis.

(The  $\rho^{(+)}$  ratio): The  $\rho^{(+)}$  ratio, the ratio of the real to imaginary part of  $F^{(+)}(\nu)$  is obtained from Eqs. (2), (5) and (6) as

$$\begin{aligned} \rho^{(+)}(\nu) &= \frac{Re \ F^{(+)}(\nu)}{Im \ F^{(+)}(\nu)} = \frac{Re \ R(\nu) + Re \ F_{P'}(\nu)}{Im \ R(\nu) + Im \ F_{P'}(\nu)} \\ &= \frac{\frac{\pi\nu}{2M^2} \left( c_1 + 2c_2 \log \frac{\nu}{M} \right) - \frac{\beta_{P'}}{M} \left( \frac{\nu}{M} \right)^{0.5}}{\frac{k\sigma_{\text{tot}}^{(+)}(\nu)}{4\pi}} . \end{aligned} \quad (10)$$

(General approach): The FESR(1)(Eq. (8)) has some problem. i.e., there are the so-called unphysical regions coming from boson poles below the  $\bar{p}p$  threshold. So, the contributions from unphysical regions of the first term of the right-hand side of Eq. (8) have to be calculated. Reliable estimates, however, are difficult. Therefore, we will not adopt the FESR(1).

On the other hand, contributions from the unphysical regions to the first term of the left-hand side of FESR(2)(Eq. (9)) can be estimated to be less than an order of 0.1% compared with the second term.<sup>1</sup> Thus, it can easily be neglected.

Therefore, the FESR(2)(Eq. (9)), the formula of  $\sigma_{\text{tot}}^{(+)}$ (Eqs. (1) and (2)) and the  $\rho^{(+)}$  ratio (Eq. (10)) are our starting points. Armed with the FESR(2), we express high-energy parameters  $c_0, c_1, c_2, \beta_{P'}$  in terms of the integral of total cross sections up to  $N$ . Using this FESR(2) as a constraint for  $\beta_{P'} = \beta_{P'}(c_0, c_1, c_2)$ , the number of independent parameters is three. We then search for the simultaneous best fit to the data points of  $\sigma_{\text{tot}}^{(+)}(k)$  and  $\rho^{(+)}(k)$  for  $70\text{GeV} \leq k \leq P_{\text{large}}$  to determine the values of  $c_0, c_1, c_2$  giving the least  $\chi^2$ . We thus predict the  $\sigma_{\text{tot}}$  and  $\rho^{(+)}$  in LHC energy and high-energy cosmic ray regions.

(Data): We use rich data[9] of  $\sigma^{\bar{p}p}$  and  $\sigma^{pp}$  to evaluate the relevant integrals of cross sections appearing in FESR(2). We connect the each data point<sup>2</sup> of  $k^2\sigma_{\text{tot}}^{\bar{p}p}$  and  $k^2\sigma_{\text{tot}}^{pp}$  with the next point by a straight line in order, from  $k = 0$  to  $k = \bar{N}$ , and regard the area of this polygonal line graph as the relevant integral in the region  $0 \leq k \leq \bar{N}$ . The integral of  $k^2\sigma_{\text{tot}}^{(+)}(k)$  is given by averaging those of  $k^2\sigma_{\text{tot}}^{\bar{p}p}(k)$  and  $k^2\sigma_{\text{tot}}^{pp}(k)$ . We have obtained

---

<sup>1</sup> The average of the imaginary part from boson poles below the  $\bar{p}p$  threshold is the smooth extrapolation of the  $t$ -channel  $qq\bar{q}\bar{q}$  exchange contributions from high energy to  $\nu \leq M$  due to FESR duality[4,5]. Since  $\text{Im } F_{qq\bar{q}\bar{q}}^{(+)}(\nu) < \text{Im } F^{(+)}(\nu)$ ,  $\int_0^M \nu \text{Im } F_{qq\bar{q}\bar{q}}^{(+)}(\nu) d\nu < \int_0^M \nu \text{Im } F^{(+)}(\nu) d\nu = \int_0^M \frac{\nu}{2} \text{Im } f^{\bar{p}p}(\nu) d\nu \simeq \frac{M^2}{4} \text{Im } f^{\bar{p}p}|_{k=0} \simeq 3.2\text{GeV} \ll \frac{1}{4\pi} \int_0^{\bar{N}} k^2 \sigma_{\text{tot}}^{(+)}(k) dk = 3403 \pm 20\text{GeV}$ , where we use the experimental value,  $\frac{k}{4\pi} \sigma_{\text{tot}}^{\bar{p}p} \simeq 14.4\text{GeV}^{-1}$  in  $k < 0.3\text{GeV}$ . So, the first term of Eq. (9) is less than 0.1% of the second term.

<sup>2</sup> We take the error  $\Delta y$  for each data point  $y$  as  $\Delta y = \sqrt{(\Delta y)_{\text{stat}}^2 + (\Delta y)_{\text{syst}}^2}$ . When several data points, denoted  $y_i$  with error  $\Delta y_i$  ( $i = 1, \dots, n$ ), are listed at the same value of  $k$ , these points are replaced by  $\bar{y}$  with  $\Delta \bar{y}$ , given by  $\bar{y} = [\sum_i y_i / (\Delta y_i)^2] / [\sum_i 1 / (\Delta y_i)^2]$  and  $\Delta \bar{y} = \sqrt{1 / [\sum_i 1 / (\Delta y_i)^2]}$ . Then, the data points with  $\Delta \bar{y}$  less than 3 mb are picked up. As a result, we obtain the 255(124) points for  $k^2\sigma_{\text{tot}}^{\bar{p}p}(k^2\sigma_{\text{tot}}^{pp})$ , giving the integrals  $(5.070 \pm 0.034) \times 10^4$  ( $(3.482 \pm 0.037) \times 10^4$ )GeV in the region  $0 \leq k \leq \bar{N}$  with  $\bar{N} = 10\text{GeV}$ .

$$\frac{1}{4\pi} \int_0^{\bar{N}} k^2 \sigma_{\text{tot}}^{(+)}(k) dk = 3403 \pm 20 \text{ GeV.} \quad (11)$$

for  $\bar{N} = 10 \text{ GeV}$  (which corresponds to  $\sqrt{s} = E_{cm} = 4.54 \text{ GeV}$ ).<sup>3</sup> The error of the integral, which is from the error of each data point, is very small (less than 1%), and thus, we regard the central value as an exact one in the following analysis.

When  $\sigma_{\text{tot}}^{\bar{p}p}$  and  $\sigma_{\text{tot}}^{pp}$  data points are listed at the same value of  $k$ , we make the  $\sigma_{\text{tot}}^{(+)}(k)$  data point by averaging these values. Totally, 37 points are obtained in the energy region,  $0.54 \text{ GeV} \leq k \leq 2100 \text{ GeV}$ . The data point of maximum value  $k = 2094.03 \text{ GeV} (\sqrt{s} = 62.7 \text{ GeV})$  comes from ISR[10]. There are 12 points in the  $70 \text{ GeV} \leq k \leq 2100 \text{ GeV}$  ( $11.5 \text{ GeV} \leq \sqrt{s} \leq 62.7 \text{ GeV}$ ). There are no data reported in the wide range of  $2100 \text{ GeV} \leq k \leq 1 \times 10^5 \text{ GeV}$ . There are 6 points[11,12] of  $\sigma_{\text{tot}}^{\bar{p}p}$  in the Tevatron-collider energy region,  $1 \times 10^5 \text{ GeV} \leq k \leq 2 \times 10^6 \text{ GeV}$ . The datum with the maximum  $k = 1.7266 \times 10^6 \text{ GeV} (\sqrt{s} = 1.8 \text{ TeV})$  in this energy range comes from Tevatron. Again there are no data reported in the range  $2 \times 10^6 \text{ GeV} \leq k \leq 2 \times 10^7 \text{ GeV}$ . There are 7 points of  $\sigma_{\text{tot}}^{pp}$  with somewhat large errors, reported in the cosmic-ray energy region,  $2 \times 10^7 \text{ GeV} \leq k \leq 5 \times 10^8 \text{ GeV}$  ( $6 \text{ TeV} \leq \sqrt{s} \leq 30 \text{ TeV}$ ), coming from cosmic-ray experiments[8]. We regard these  $\sigma_{\text{tot}}^{\bar{p}p}$  and  $\sigma_{\text{tot}}^{pp}$  data as  $\sigma_{\text{tot}}^{(+)}$  data points. Totally we obtain 25 points of  $\sigma_{\text{tot}}^{(+)}$  in  $k \geq 70 \text{ GeV}$ , which are used in the analyses.

The data of  $\rho^{\bar{p}p}(k) (= \text{Re } f^{\bar{p}p}(k) / \text{Im } f^{\bar{p}p}(k))$  and  $\rho^{pp}(k) (= \text{Re } f^{pp}(k) / \text{Im } f^{pp}(k))$  are reported in ref.[9]. When both data points are listed at the same value of  $k$ , we can make the  $\rho^{(+)}(k) (= \text{Re } F^{(+)}(k) / \text{Im } F^{(+)}(k))$  data point.<sup>4</sup> We obtain 9 points of  $\rho^{(+)}$  in the energy region,  $70 \text{ GeV} \leq k \leq 2100 \text{ GeV}$ .<sup>5</sup> No data are reported in the range  $2100 \text{ GeV} \leq k \leq 1 \times 10^5 \text{ GeV}$ . The two points of  $\rho^{\bar{p}p}$  are reported in Tevatron-collider energy region,  $1 \times 10^5 \text{ GeV} \leq k \leq 2 \times 10^6 \text{ GeV}$  (at  $k = 1.5597 \times 10^5 \text{ GeV} (\sqrt{s} = 541 \text{ GeV})$ [14] and  $k = 1.7266 \times 10^6 \text{ GeV} (\sqrt{s} = 1.8 \text{ TeV})$ [15]). We regard these two points as the  $\rho^{(+)}$  data. As a result, we obtain 11 points of  $\rho^{(+)}$  up to Tevatron-collider energy

<sup>3</sup> The laboratory momentum  $P_{lab}$  are related to the CM energy squared  $s$  by  $s = 2M(M + \sqrt{M^2 + P_{lab}^2})$  and equivalently  $P_{lab} = \frac{s}{2M} \sqrt{1 - 4M^2/s}$ . Thus, at high energies  $E_{cm} = \sqrt{s} \simeq \sqrt{2MP_{lab}}$ .

<sup>4</sup> Here the values of  $\text{Im } f^{\bar{p}p}(k)$  and  $\text{Im } f^{pp}(k)$  at the relevant values of  $k$  are determined through the formula given in ref.[9],  $\sigma^{\bar{p}p/pp} = Z + B \log^2(s/s_0) + Y_1(s_1/s)^{\eta_1} \pm Y_2(s_1/s)^{\eta_2}$  with  $(Z, B, Y_1, Y_2) = (35.45, 0.308, 42.53, 33.34) \text{ mb}$ ,  $(\sqrt{s_0}, \sqrt{s_1}) = (5.38, 1) \text{ GeV}$  and  $(\eta_1, \eta_2) = (0.458, 0.545)$ .

<sup>5</sup> Here only the data point of maximum  $k = 1479 \text{ GeV} (\sqrt{s} = 52.7 \text{ GeV})$  is obtained by combining the  $\rho^{\bar{p}p}$  at  $k = 1473.46 \text{ GeV} (\sqrt{s} = 52.6 \text{ GeV})$  and  $\rho^{pp}$  at  $k = 1484.69 \text{ GeV} (\sqrt{s} = 52.8 \text{ GeV})$ , reported in ref.[13]. The other 8 points are obtained by combining  $\rho^{\bar{p}p}$  and  $\rho^{pp}$  with the same values of  $k$ .

Table 1

The values of  $\chi^2$  for the fit 1 (fit up to ISR energy) and the fit 2 (fit up to Tevatron-collider energy).  $N_F$  and  $N_\sigma(N_\rho)$  are the degree of freedom and the number of  $\sigma_{\text{tot}}^{(+)}(\rho^{(+)})$  data points in the fitted energy region.

	$\chi^2/N_F$	$\chi^2/N_\sigma$	$\chi^2/N_\rho$
fit 1	10.6/15	3.6/12	7.0/7
fit 2	13.6/23	6.0/18	7.6/9

region,  $70\text{GeV} \leq k \leq 2 \times 10^6\text{GeV}$ .

In the actual analyses, we use  $\text{Re } F^{(+)}$  instead of  $\rho^{(+)}$  ( $= \text{Re } F^{(+)} / \text{Im } F^{(+)}$ ). The data points of  $\text{Re } F^{(+)}(k)$  are made by multiplying  $\rho^{(+)}(k)$  by  $\text{Im } F^{(+)}(k) = \frac{k}{8\pi}(\sigma_{\text{tot}}^{\bar{p}p}(k) + \sigma_{\text{tot}}^{pp}(k))$ . The values of  $\sigma_{\text{tot}}^{\bar{p}p}$  and  $\sigma_{\text{tot}}^{pp}$  at the relevant values of  $k$  are obtained as follows: For  $k < 1500\text{GeV}$ , they are determined by the formula given in ref.[9](see the footnote 4). Two experimental values[12] of  $\sigma^{\bar{p}p}$  in the Tevatron region are used.

(Analysis): As was explained in the general approach, both  $\sigma_{\text{tot}}^{(+)}$  and  $\text{Re } F^{(+)}$  data in  $70\text{GeV} \leq k \leq P_{\text{large}}$  are fitted simultaneously through the formula Eq. (2) and Eq. (10) with the FESR(2)(Eq. (9)) as a constraint. FESR(2) with Eq. (11) gives us

$$8.87 = c_0 + 2.04c_1 + 4.26c_2 + 0.367\beta_{P'} , \quad (12)$$

which is used as a constraint of  $\beta_{P'} = \beta_{P'}(c_0, c_1, c_2)$ , and the fitting is done by three parameters  $c_0, c_1$  and  $c_2$ .

We have done for the following two cases:

**fit 1**): The fit to the data up to ISR energy region,  $70\text{GeV} \leq k \leq 2100\text{GeV}$ , which includes 12 points of  $\sigma_{\text{tot}}^{(+)}$  and 7 points of  $\rho^{(+)}$ .

**fit 2**): The fit to the data up to Tevatron-collider energy region,  $70\text{GeV} \leq k \leq 2 \times 10^6\text{GeV}$ , which includes 18 points of  $\sigma_{\text{tot}}^{(+)}$  and 9 points of  $\rho^{(+)}$ .

(Results of the fit): The results are shown in Fig. 1(Fig. 2) for the fit 1(fit 2). The  $\chi^2/d.o.f = 10.6/15$  (13.6/23) in the fit 1 (fit 2) are given in Table 1. The respective  $\chi^2$ -values devided by the number of data points for  $\sigma_{\text{tot}}^{(+)}$  and  $\rho^{(+)}$  are less than or equal to unity. The fits are successful in both cases.

The best-fit values of the parameters are given in Table 2. Here the errors of one standard deviation are also given.<sup>6</sup>

<sup>6</sup> The  $c_2 \log^2(\nu/M)$ -term in Eq. (2) is most relevant for predicting  $\sigma_{\text{tot}}^{(+)}$  in high energy region, and thus, the error estimation is done as follows: The  $c_2$  is fixed with a value deviated a little from the best-fit value, and then the  $\chi^2$ -fit is done by two parameters  $c_0$  and  $c_1$ . When the resulting  $\chi^2$  is larger than the least  $\chi^2$

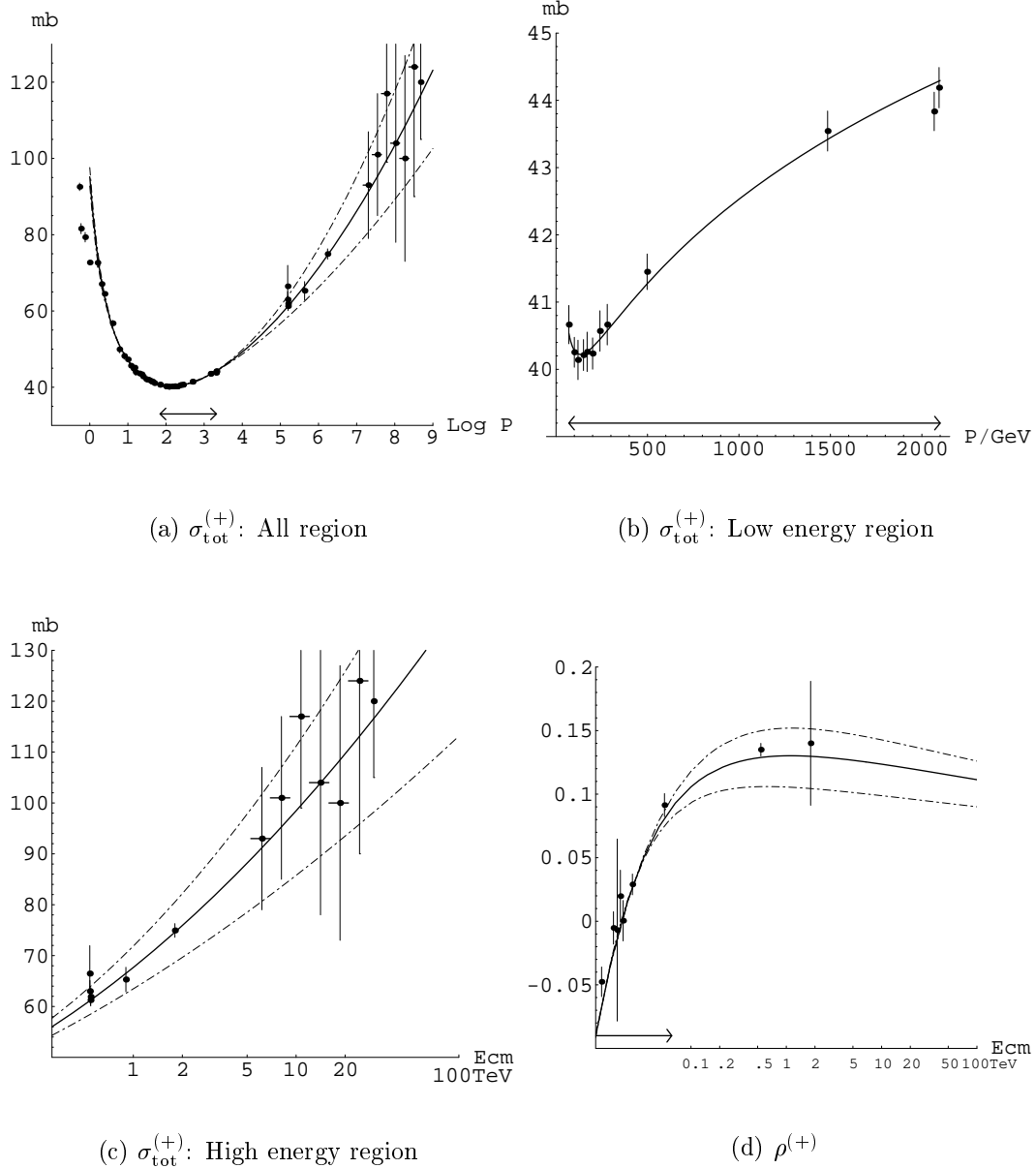


Fig. 1. Predictions for  $\sigma^{(+)}$  and  $\rho^{(+)}$  in terms of the fit 1. The fit is done for the data up to the ISR energy, in the region  $70\text{GeV} \leq k \leq 2100\text{GeV}$  ( $11.5\text{GeV} \leq \sqrt{s} \leq 62.7\text{GeV}$ ) which is shown by the arrow in each figure. Total cross section  $\sigma_{\text{tot}}^{(+)}$  in (a) all energy region, versus  $\log_{10} P_{\text{lab}}/\text{GeV}$ , (b) low energy region (up to ISR energy), versus  $P_{\text{lab}}/\text{GeV}$  and (c) high energy (Tevatron-collider, LHC and cosmic-ray energy) region, versus center of mass energy  $E_{\text{cm}}$  in TeV unit. (d) gives the  $\rho^{(+)}$  ( $= \text{Re } F^{(+)} / \text{Im } F^{(+)}$ ) in high energy region, versus  $E_{\text{cm}}$  in terms of TeV. The thin dot-dashed lines represent the one standard deviation.

(Predictions for  $\sigma^{(+)}$  and  $\rho^{(+)}$  at LHC and cosmic-ray energy region): By us-

---

of the three-parameter fit by one, the corresponding values of parameters give one standard deviation.

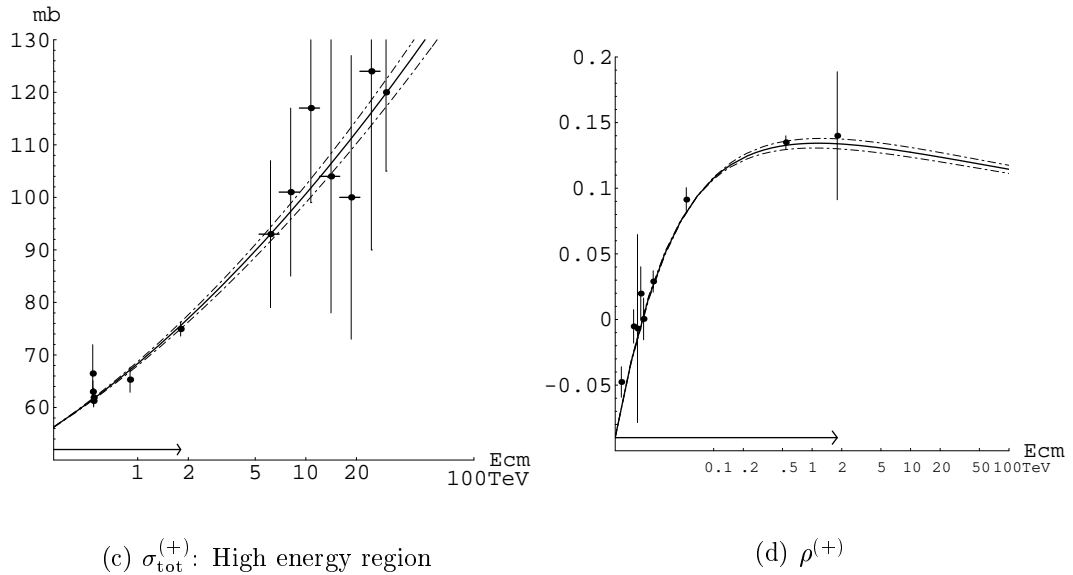
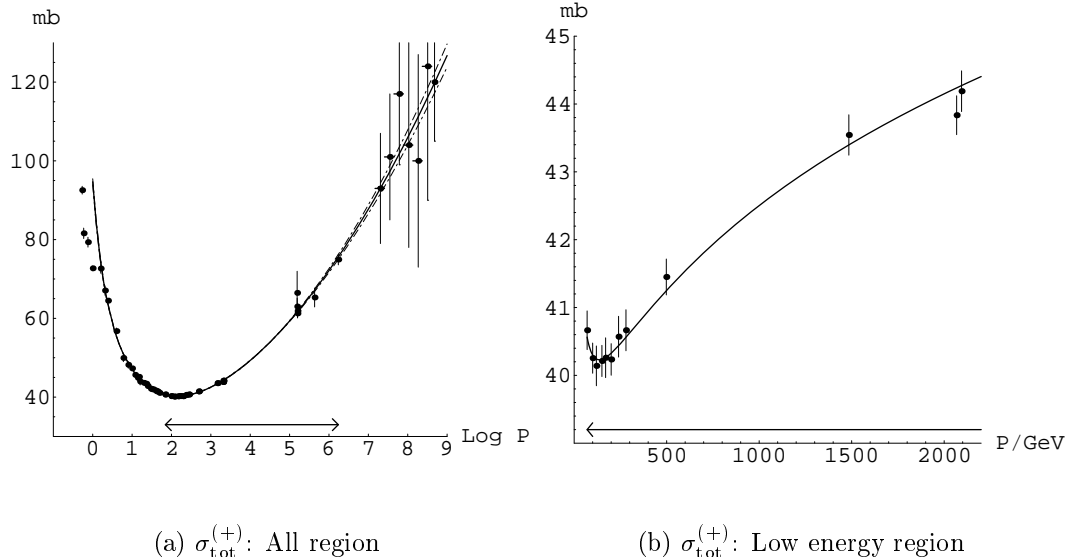


Fig. 2. Predictions for  $\sigma^{(+)}$  and  $\rho^{(+)}$  in terms of the fit 2. The fit is done for the data up to Tevatron-collider energy, in the region  $70\text{GeV} \leq k \leq 2 \times 10^6\text{GeV}$  ( $11.5\text{GeV} \leq \sqrt{s} \leq 1.8\text{TeV}$ ) which is shown by the arrow. For each figure, see the caption in Fig.1.

Table 2

The best-fit values of parameters in the fit 1 and the fit 2.

	$c_2$	$c_1$	$c_0$	$\beta_{P'}$
fit 1	$0.0411 \pm 0.0199$	$-0.074 \mp 0.287$	$5.92 \pm 1.07$	$7.96 \mp 1.55$
fit 2	$0.0448 \pm 0.0037$	$-0.128 \mp 0.063$	$6.13 \pm 0.26$	$7.66 \mp 0.41$

Table 3

The predictions of  $\sigma_{\text{tot}}^{(+)}$  and  $\rho^{(+)}$  at LHC energy  $\sqrt{s} = E_{cm} = 14\text{TeV}$  ( $P_{lab}=1.04 \times 10^8 \text{GeV}$ ), and at a very high energy  $P_{lab} = 5 \cdot 10^{20} \text{eV}$  ( $\sqrt{s}=E_{cm}=967\text{TeV}$ ) in cosmic-ray region.

	$\sigma_{\text{tot}}^{(+)}$ ( $\sqrt{s}=14\text{TeV}$ )	$\rho^{(+)}$ ( $\sqrt{s}=14\text{TeV}$ )	$\sigma_{\text{tot}}^{(+)}$ ( $P_{lab}=5 \cdot 10^{20} \text{eV}$ )	$\rho^{(+)}$ ( $P_{lab}=5 \cdot 10^{20} \text{eV}$ )
fit 1	$103.8 \pm 14.3 \text{mb}$	$0.122^{+0.018}_{-0.024}$	$188 \pm 43 \text{mb}$	$0.099^{+0.011}_{-0.017}$
fit 2	$106.3 \pm 1.9 \text{mb}$	$0.126 \pm 0.004$	$196.2 \pm 6.8 \text{mb}$	$0.102 \pm 0.002$

ing the values of parameters in Table 2, we can predict the  $\sigma_{\text{tot}}^{(+)}$  and  $\rho^{(+)}$  in higher energy region, as are shown, respectively in (c) and (d) of Fig. 1 and 2. The thin dot-dashed lines represent the one standard deviation.

As is seen in (c) and (d) of Fig. 1, the fit 1 leads to the prediction of  $\sigma_{\text{tot}}^{(+)}$  and  $\rho^{(+)}$  with somewhat large errors in the Tevatron-collider energy region, although the best-fit curves are consistent with the present experimental data in this region. Furthermore, the predicted values of  $\sigma_{\text{tot}}^{(+)}$  agree with  $pp$  experimental data at the cosmic-ray energy regions[8] within errors (see (a),(c) of Fig. 1). The best-fit curve gives  $\chi^2/(\text{number of data})$  to be 5.8/15, and the prediction is successful. As was mentioned in the purpose of this Letter, it has to be noted that the energy range of predicted  $\sigma_{\text{tot}}^{(+)}$  is several orders of magnitude larger than the energy region of the  $\sigma_{\text{tot}}^{(+)}, \rho^{(+)}$  input. If we use data up to Tevatron-collider energy region as in the fit 2, the situation is much improved (see (a),(c) of Fig. 2). The best-fit curve gives  $\chi^2/(\text{number of data})$  from cosmic-ray data, 1.0/7.

We can predict the values of  $\sigma_{\text{tot}}^{(+)}$  and  $\rho^{(+)}$  at LHC energy,  $\sqrt{s}=E_{cm}=14\text{TeV}$  and at very high energy of cosmic-ray region. The relevant energies are very high, and the  $\sigma_{\text{tot}}^{(+)}$  and  $\rho^{(+)}$  can be regarded to be equal to the  $\sigma_{\text{tot}}^{pp}$  and  $\rho^{pp}$ . The results are shown in Table 3.

Table 3 is instructive. The prediction by the fit 1 in which data up to the ISR energy are used as input has somewhat large(fairly large) errors at LHC energy(at high energy of cosmic ray). By including the data up to the Tevatron collider as in the prediction by the fit 2, the errors at LHC energy become very small although these are still somewhat large in high-energy region of cosmic ray.

Using the data up to  $\sqrt{s} = 1.8\text{TeV}$ (Tevatron), we can predict the  $\sigma_{\text{tot}}^{pp}$  and  $\rho^{pp}$  at LHC energy( $\sqrt{s} = E_{cm} = 14\text{TeV}$ ) as  $106.3 \pm 1.9 \text{mb}$  and  $0.126 \pm 0.004$ , respectively (see Table 3).

Finally we emphasize that it is quite important to measure both  $\sigma_{\text{tot}}^{pp}$  and  $\rho^{pp}$  precisely in the coming LHC experiment in order to investigate  $\sigma^{pp}$  and  $\rho^{pp}$  in the extremely high-energy regions more than  $5 \times 10^{20} \text{eV}$ .

## References

- [1] K. Igi and M. Ishida, Phys. Rev. D 66 (2002) 034023.
- [2] J. R. Cudell et al., Phys. Rev. D 61 (2000) 034019.
- [3] K. Igi, Phys. Rev. Lett. 9 (1962) 76.
- [4] K. Igi and S. Matsuda, Phys. Rev. Lett. 18 (1967) 625.
- [5] R. Dolen, D. Horn and C. Schmid, Phys. Rev. 166 (1968) 1768. This paper includes references on earlier papers on FESR.
- [6] M. Froissart, Phys. Rev. 123 (1961) 1053.  
A. Martin, Nuovo Cim. 42 (1966) 930.
- [7] M. M. Block and F. Halzen, Phys. Rev. D 70 (2004) 091901.
- [8] M. Honda et al., Phys. Rev. Lett. 70 (1993) 525.  
R. M. Baltrusaitis et al., Phys. Rev. Lett. 52 (1984) 1380.
- [9] Particle Data Group, S. Eidelman et al., Phys. Lett. B 592 (2004) 313.
- [10] G. Carboni et al., Nucl. Phys. B 254 (1984) 697.  
U. Amaldi et al., Nucl. Phys. B 145 (1978) 367.
- [11] G. Arnison et al., UA1 Collaboration, Phys. Lett. B 128 (1983) 336.  
R. Battiston et al., UA4 Collaboration, Phys. Lett. B 117 (1982) 126.  
M. Bozzo et al., UA4 Collaboration, Phys. Lett. B 147 (1984) 392.  
G. J. Alner et al., UA5 Collaboration, Zeit. Phys. C 32 (1986) 153.
- [12] C. Augier et al., Phys. Lett. B 344 (1995) 451.  
F. Abe et al., CDF Collaboration, Phys. Rev. D 50 (1994) 5550.  
C. Avila et al., E-811 Collaboration, Phys. Lett. B 445 (1999) 419.  
N. A. Amos et al., E-710 Collaboration, Phys. Rev. Lett. 68 (1992) 2433.
- [13] N. Amos et al., Nucl. Phys. B 262 (1985) 689.
- [14] C. Augier et al., Phys. Lett. B 316 (1993) 448.
- [15] N. A. Amos et al., E-710 Collaboration, in ref.[12].